DOI 10.1002/pmic.201000228 *Proteomics* 2010, *10*, 4320–4334

DATASET BRIEF

Quantitative proteomic analysis of A549 cells infected with human respiratory syncytial virus subgroup B using SILAC coupled to LC-MS/MS

Diane C. Munday[1], *Julian A. Hiscox*[1,2] *and John N. Barr*[1,2]

[1] Institute of Molecular and Cellular Biology, Faculty of Biological Sciences, University of Leeds, Leeds, UK
[2] Astbury Centre for Structural Molecular Biology, University of Leeds, Leeds, UK

Received: April 7, 2010
Revised: July 1, 2010
Accepted: August 31, 2010

Human respiratory syncytial virus (HRSV) is a leading cause of serious lower respiratory tract infections in infants. The virus has two subgroups A and B, which differ in prevalence and (nucleotide) sequence. The interaction of subgroup A viruses with the host cell is relatively well characterized, whereas for subgroup B viruses it is not. Therefore quantitative proteomics was used to investigate the interaction of subgroup B viruses with A549 cells, a respiratory cell line. Changes in the cellular proteome and potential canonical pathways were determined using SILAC coupled to LC-MS/MS and Ingenuity Pathway Analysis. To reduce sample complexity and investigate potential trafficking both nuclear and cytoplasmic fractions were analyzed. A total of 904 cellular and six viral proteins were identified and quantified, of which 112 cellular proteins showed a twofold or more change in HRSV-infected cells. Data sets were validated using indirect immunofluorescence confocal microscopy on independent samples. Major changes were observed in constituents of mitochondria including components of the electron transport chain complexes and channels, as well as increases in the abundance of the products of interferon-stimulated genes. This is the first quantitative proteomic analysis of cells infected with HRSV-subgroup B.

Keywords:
Bioinformatics / Fluorescent labeling / Global protein analysis / Microbiology
Western blots

Human respiratory syncytial virus (HRSV) is a leading cause of serious lower respiratory tract infection in infants [1]. HRSV belongs in the *Paramyxoviridae* family (order *Mononegavirales*), which includes other viruses such as parainfluenza virus, human metapneumovirus and measles virus (MV). Two subgroups of HRSV have been identified (A and B), which generally share 81% genomic nucleotide homology and 88% aggregate proteome amino acid sequence identity. Between subgroup A and B, all viral proteins exhibit a degree of amino acid identity divergence, but some proteins exhibit this to a greater extent, such as M2-2 (72%), which is involved in modulating viral RNA synthesis [2], the small hydrophobic protein (SH [76%]), which is a viroporin [3], and the glycoprotein (G [53%]), which is responsible for receptor recognition and attatchment [4]. Arguably the best-studied variants are subgroup A viruses. No vaccine or effective therapeutic treatment currently exists, and anti-viral therapy is licensed only for the immunoprophylactic treatment of high-risk infants [5]. A better understanding of the interaction between HRSV and the host cell at the molecular level is essential for the development of new therapeutic strategies [6]. Two approaches for achieving this are transcriptomics and proteomics.

During infection of model cell lines with HRSV subgroup A, transcriptomic analysis revealed that the virus had multiple effects on the host cell including upregulation

Correspondence: Dr. John N. Barr, Garstang Building, Institute of Molecular and Cellular Biology, Faculty of Biological Sciences, University of Leeds, Leeds LS2 9JT, UK
E-mail: j.n.barr@leeds.ac.uk
Fax: +44-113-343-3115

Abbreviations: HRSV, human respiratory syncytial virus; **VDAC,** voltage-dependent anion channel

of immune response genes including antigen processing and interferon stimulated genes, upregulation of the urokinase plaminogen activator and urokinase plaminogen activator receptor system, apoptotic pathways and genes involved in the organization of the cytoskeleton [7, 8]. The onset of gene induction can be temporally regulated and in general gene upregulation was greater than downregulation [7]. Proteomics using 2-DE has been applied previously to study the interaction between HRSV subgroup A and the host-cell nuclear [9] and total cell proteomes [10], where the abundance of 24 and 21 proteins, respectively, were shown to change. Areas of commonality included the induction of proteins involved in the stress response.

Specific canonical and signaling pathways have also been investigated in subgroup A-infected cells [6], including cell cycle arrest through the upregulation of transforming growth factor β1 [11], alteration of lipid raft membrane composition [12], decreases in components of the interferon pathways such as TRAF3 and STAT2 [13], activation of the NF-κB signal transduction pathway [14, 15] and activation of innate immunity through Toll-like receptor 2 [16]. Many of these processes are regulated by the induction of different cellular gene subsets highlighted in the transcriptomic analyses [8, 17].

In contrast, very little is known about how subgroup B viruses interact with the host cell and this was the focus of this study. The elucidation of proteomic changes in cells infected with this subgroup would provide both a valuable data set, and more importantly, a point of comparison with the better characterized subgroup A viruses. Such studies may also help to identify common host-cell responses, and mechanisms used by viruses with different replication strategies, thus providing information on how the metabolic profile of a cell changes in response to infection and inform as to potential therapeutic targets.

To globally assess changes in the proteome of cells infected with HRSV subgroup B, SILAC coupled to LC-MS/MS for protein identification and quantification was used [18, 19]. To reduce sample complexity and to study the interaction of HRSV with different cellular compartments, nuclear and cytoplasmic fractions were purified and analyzed separately. A549 cells, a human lung carcinoma cell line that retains properties of HRSV-permissive alveolar cells, were used in this study. Due to its respiratory origin, this cell line has been extensively used in the characterization of HRSV-infection and in the proteomic analysis of cellular and infectious respiratory diseases [9, 10, 20–22]. Mock-infected cells were grown in media labeled with R6K4 (Dundee Cell Products) and cells infected with subgroup B virus (at a multiplicity of infection of 1) were grown in media containing R0K0. Nuclear and cytoplasmic fractions were harvested 24 h post-infection. This time point was chosen to compare to other proteomic and transcriptomic analysis of HRSV-infected cells and also to ensure that the cells were approximately 75% confluent and not undergoing contact inhibition. In addition, at this multiplicity of infection and time point, little sign of cell death was apparent, probably reflecting that HRSV can delay apoptosis under certain conditions [23, 24]. Cell pellets were re-suspended in a cold cytoplasmic lysis buffer (20 mM Tris-HCl (pH 7.5), 100 mM NaCl, 0.5 mM EDTA 0.5% NP-40, EDTA-free complete protease inhibitor mixture (Roche)) and incubated for 10 min on ice. The supernatant containing predominantly cytoplasmic proteins was collected after a 3-min centrifugation at 2000 × *g* at 4°C. The remaining pellet was re-suspended in RIPA buffer (50 mM Tris, pH 7.5, 150 mM NaCl, 1% NP40, 0.5% sodium deoxycholate 0.1% SDS, EDTA-free complete protease inhibitor mixture (Roche)) and incubated for 30 min at 4°C. The supernatant containing predominantly total soluble nuclear protein was collected after a 2-min centrifugation at 13 000 × *g* at 4°C. Both fractions were incubated for 5 min at 4°C in a sonicating water bath. The quality of the nuclear and cytoplasmic fractions was surveyed using specific markers to cellular and viral proteins (Supporting Information Fig. 1). The data indicated that enriched nuclear and cytoplasmic fractions were obtained, and suggested that potential changes in the abundance of cellular proteins occurred in HRSV-infected cells. For example, a decrease in the abundance of the nuclear/nucleolar protein, nucleolin, was observed in the nuclear fraction (Supporting Information Fig. 1).

Each cytoplasmic and nuclear fraction from mock-infected and HRSV-infected cells was combined and the proteins separated by SDS-PAGE (4–12% Bis-Tris Novex mini-gel, Invitrogen). Ten gel slices *per* fraction were extracted and subjected to in-gel digestion using trypsin. Purified peptides were separated using an Ultimate U3000 (Dionex), trap-enriched nanoflow LC-system and identified using an LTQ Orbitrap XL (Thermo Fisher Scientific) *via* a nano ES ion source (Proxeon Biosystems) by Dundee Cell Products. Quantification was performed with MaxQuant version 1.0.7.4 [25] and was based on 2-D centroid of the isotope clusters within each SILAC pair. The generation of the peak list, SILAC and extracted ion current-based quantification, calculation of posterior error probability, as well as the false discovery rate (based on search engine results), peptide to protein group assembly, data filtration and presentation were carried out using MaxQuant. The derived peak list was searched with the Mascot search engine (version 2.1.04; Matrix Science, London, UK) against a concatenated database combining 80 412 proteins from the International Protein Index human protein database version 3.6 (forward database), and the reversed sequences of all proteins (reverse database). Full methodology for the SILAC coupled to the LC-MS/MS analysis to study virus/host interactions has been described previously [18, 19].

For quantitative analysis, previous investigations using SILAC and LC-MS/MS have applied fold-change cutoffs ranging from 1.3- to 2.0-fold [26]. In this study, a 2.0-fold cutoff was chosen as a basis for investigating potential proteome changes between data sets using Ingenuity Pathway Analysis, and to provide a basis for comparing the current data set to previous HRSV and other virus studies that have used this delineator [17, 27]. Cellular and viral proteins were identified and quantified in the nuclear and

cytoplasmic fractions and raw data sets were deposited in the PRIDE [28] using the PRIDE convertor tool [29]. In the nuclear and cytoplasmic fractions, 464 and 440 cellular proteins were identified and quantified, respectively. Of these, 123 proteins (Table 1) between the different fractions showed a difference in abundance of twofold or greater, which represented 112 unique proteins (as some proteins were present in both fractions). Mitochondrial proteins are a known contaminant of nuclear fractions [22] and are presented separately in Table 1 because of this. Several viral proteins were also identified in the nuclear (nucleoprotein (N), phosphoprotein (P), non-structural protein 1 (NS1), matrix (M) protein and M2-1 protein) fraction (Supporting Information Table 1) and the cytoplasmic fraction (N, P, NS1, M2-1, M and fusion (F) protein) (Supporting Information Table 2).

Ingenuity Pathway Analysis was used to examine the cellular protein data sets and to group proteins into similar functional classes. Pathway analysis highlighted several protein networks and canonical pathways that were potentially altered in HRSV-infected cells, based upon underlying biological evidence from the curated Ingenuity literature database. For the proteins that were differentially regulated in the nuclear (excluding mitochondrial proteins) and cytoplasmic fractions, the number of proteins assigned to different functional categories are shown in Fig. 1A. For example, 20 proteins involved in cell death showed a twofold or more decrease in the nucleus fraction in virus-infected cells (p-value 1.44×10^{-5} to 4.88×10^{-2}). Other major changes were observed in pathways involved in cell morphology, cellular assembly and organization, protein degradation and gene expression (Fig. 1A). This is similar to other quantitative proteomic analyses of virus-infected cells using SILAC coupled to LC-MS/MS. Such studies have focused on coronavirus- [18], influenza virus- [20, 30] and HIV-1 [31] infected cells.

Several canonical pathways were potentially altered in HRSV-infected cells including interferon signaling (p-value 1.97×10^{-5}) (Fig. 1B). STAT1 was increased 6.3-fold. This protein mediates the expression of a variety of genes considered central to the host-cell response to infection or inflammation. Examples of such proteins identified in this study included interferon-induced protein with tetratricopeptide repeats 1 (IFIT1) (increased 8.9-fold in HRSV-infected cells) and myxovirus (influenza virus) resistance 1 interferon-inducible protein p78 (MX1) (increased 11.2-fold in HRSV-infected cells) (Fig. 1B). The observed increase in STAT1 in HRSV-infected cells has been shown previously in human diploid fibroblast 2fTGH cells, which were infected with HRSV subgroup A [32]. Likewise, the increased expression of *MX1* mRNA and protein has been demonstrated in tissues isolated from cotton rats infected with HRSV subgroup A [33]. In the current data set, pathway analysis linked these molecules to NF-κB activated transcription and IFNα/β (*e.g.* Fig. 1B), all of which have been described in HRSV subgroup A-infected cells [11, 14, 34]. Therefore, previously published data were reflected by the bioinformatic analysis of the quantitative proteomic data. However, there have been differing reports of the effect of different HRSV subgroup A viruses on inducing interferon type I. Similar to a micro-array analysis of A549 cells infected with HRSV subgroup A [7], the quantitative proteomic analysis supports the activation of interferon stimulated genes in A549 cells infected with subgroup B virus.

One of the novel findings of this quantitative proteomic analysis was the alteration of mitochondrial proteins in HRSV-infected cells. The abundance of proteins associated with respiratory complexes 1, 3, 4 and 5 (Supporting Information Fig. 2), oxidative phosphorylation (Supporting Information Fig. 3), super-oxide dismutase, proteins involved in mitochondrial integrity (prohibitin) and transition pore complexes (voltage-dependent anion channels (VDACs)) were changed. As a result, Ingenuity Pathway Analysis predicted mitochondrial dysfunction in HRSV-infected cells (p-value 2.22×10^{-2}). Although it is known that mitochondria play a central role in the host-cell response to microbial infection, the change in abundance of mitochondrial proteins in HRSV-infected cells has not been previously described, and may be linked to the induction of ROS [35, 36].

The major responses to virus-infection can be directed by innate and adaptive immunity and clearly these pathways are activated in HRSV-infected cells [6, 7, 10]. More subtle specific host-cell proteins can exhibit anti-viral activity. One such protein is ADAR, an interferon inducible RNA editing enzyme, which functions to deaminate adenosine to inosine, and whose activity may depend on subcellular localization [37]. ADAR increases 2.8-fold in the nucleus in HRSV-infected cells (Table 1). ADAR has been reported to have a potential role in innate anti-viral immunity, including influenza A virus [38, 39]. Conversely, ADAR1 has been reported to act as a pro-viral, anti-apoptotic host factor in measles virus-infected cells [40] and also in cells infected with vesicular stomatitis virus [41], which also belongs to the Mononegavirales. Similarly, 2′-5′-oligoadenylate synthetase 3 was shown to increase 5.0- and 3.5-fold in the nucleus and cytoplasm of HRSV-infected cells, respectively. This protein has anti-viral activity and is activated by interferon [42, 43] and has been shown to be a part of interferon-γ-mediated inhibition of HRSV [44].

Information from the Ingenuity database and an examination of the existing literature was used to prioritize the pathway-associated proteins of interest for validation. To that end, experiments using indirect immunofluorescence confocal microscopy were used, providing a complete and independent verification of the results as this technique does not rely on subcellular fractionation and purification of proteins from mock- or HRSV-infected cells. Also, the study would provide confidence in the proteomic data set as this was from a single experiment. Microscopy analysis of the subcellular localization of Tom22, VDAC1 and prohibitin in HRSV-infected cells (compared with mock-infected cells),

Table 1. Proteins identified by LC-MS/MS demonstrating a ≥twofold change in abundance in HRSV-infected A549 cells

Protein IDs	Protein name	Gene name	RSV/Mock	Pep.	Seq. cov. (%)	PEP	Notes
Nuclear fraction – proteins that show increase abundance in RSV infected cells							
IPI00398625.5	Hornerin	HRNR	+10.0	2	5.2	8.6E−26	Potential role in cornification of the epidermis
IPI00003935.6	Histone H2B type 2-E	HIST2H2BE	+7.6	10	40.5	5.5E−33	Responsible for nucleosome structure
IPI00020101.9	Histone H2B type 1-C/E/F/G/	HIST1H2BC	+7.2	12	40.5	4.2E−33	Responsible for nucleosome structure
IPI00902514.1	Histone H2A	H2AFX	+5.6	27	20.7	1.1E−23	Responsible for nucleosome structure
IPI00877174.1	cDNA FLJ78682, highly similar to Homo sapiens 2′-5′-oligoadenylate synthetase 3, 100kDa (OAS3), mRNA; 2′-5′-oligoadenylate synthetase 3	OAS3 (includes EG:4940)	+5.0	2	3.9	3.9E−07	The mRNA for OAS2 is upregulated 4.5-fold in HRSV subgroup A infected cells at 24 h p.i. [7] and also upregulated in infected mice [50]. This protein has anti-viral activity and can promote mRNA destabilization and rRNA cleavage. (Also discussed in text.)
IPI00152503.1	Protein deltex-3-like	DTX3L	+4.9	2	5.7	0.00008	Functions as E3 ligase on capacity for self-ubiquitination
IPI00218475.4	Interferon-induced 35 kDa protein	IFI35	+4.3	2	12.8	5.3E−06	mRNA is upregulated in infection of mice with HRSV subgroup A [50]
IPI00749005.2	Nesprin-1	SYNE1	+3.7	7	0.2	0.00695	Nuclear envelope spectrin repeat proteins are located primarily in the outer nuclear membrane
IPI00299149.1	Small ubiquitin-related modifier 2	SUMO2 (includes EG:6613)	+3.2	16	29.5	1.8E−19	Post-translational modification involved in protein stability, transcriptional regulation, apoptosis and nuclear transport
IPI00102685.1	Myeloid-associated differentiation marker	MYADM	+3.2	6	10.2	2.4E−28	Localized to the nuclear envelope
IPI00291215.6	Poly [ADP-ribose] polymerase 14	PARP14	+3.2	5	1.7	8.3E−13	Linked to transcriptional regulation, genome organization and DNA-repair
IPI00418471.6	Vimentin	VIM	+2.9	7	76.2	0	Intermediate filament and component of the cytoskeleton, altered in many virus-infected cells including coronaviruses [18] and African swine fever virus [51]
IPI00394668.1	Double-stranded RNA-specific adenosine deaminase	ADAR	+2.8	5	17.8	1.3E−75	Role in RNA editing. Also discussed in text
IPI00027898.3	Uncharacterized protein C21orf70	C21ORF70	+2.8	3	13.9	8.0E−07	Unknown function
IPI00020928.1	Transcription factor A, mitochondrial	TFAM	+2.7	3	35.4	1.8E−69	Involved in mitochondrial transcription and genome replication
IPI00440688.4	Polymerase δ-interacting protein 3	POLDIP3	+2.6	3	8.2	1.4E−11	Enhances translation of spliced over non-spliced mRNAs
IPI00871695.1	Protein DEK	DEK	+2.5	3	16.5	7.7E−19	Involved in splice site selection
IPI00060181.1	EF-hand domain-containing protein D2	EFHD2	+2.4	2	17.1	1.7E−35	May regulate NF-κB canonical pathway
IPI00182757.10	Protein KIAA1967	KIAA1967	+2.4	2	34.1	1.9E−184	Inhibitor of SIRT1 which deacetylates histones and p53
IPI00465248.5	α-Enolase	ENO1	+2.2	3	20	6.2E−80	Glycolytic enzyme
IPI00024620.6	Enhancer of yellow 2 transcription factor homolog	ENY2	+2.2	6	32.7	0.00005	Involved in histone acetylation and deubiquitination
Nuclear fraction – proteins that show decreased abundance in RSV infected cells							
IPI00017334.1	Prohibitin	PHB	−12.1	7	54	1.5E−82	Involved in transcription regulation and potential chaperone for respiration chain proteins in the mitochondria. Altered in influenza virus infected cells [30]
IPI00413108.4	Putative uncharacterized protein RPSAP18	RPSAP18	−9.1	11	25.3	8.8E−15	Unknown function

Table 1. Continued

Protein IDs	Protein name	Gene name	RSV/Mock	Pep.	Seq. cov. (%)	PEP	Notes
IPI00023001.2	UPF0389 protein FAM162A	FAM162A	−9.1	2	18.8	8.8E−08	Membrane protein
IPI00647915.1	Transgelin-2	TAGLN2	−5.6	7	30	6.9E−35	Actin cross-linking protein involved in calcium interactions and regulates contractile properties
IPI00376005.2	Eukaryotic translation initiation factor 5A-1	EIF5A	−5.5	5	23.9	1.1E−63	Involved in translation elongation.
IPI00641950.3	Guanine nucleotide-binding protein subunit β-2-like 1	GNB2L1	−5.4	5	16.4	2.0E−41	Potentially binds activated protein kinase C to the cytoskeleton
IPI00012855.1	Trans-membrane protein 11	TMEM11	−5.0	2	12.5	1.6E−05	Unknown function
IPI00299024.9	Brain acid soluble protein 1	BASP1	−5.0	2	78.4	9.9E−42	Membrane-attached signal protein.
IPI00021805.1	Microsomal glutathione *S*-transferase 1	MGST1	−4.6	3	27.1	1.0E−57	Mediates inflammation. mRNA is downregulated in hMPV-infected cells [52]
IPI00472939.2	Signal peptidase complex subunit 2	SPCS2	−3.9	6	12.8	1.0E−11	Involved in translocation of polypeptide chains across the ER
IPI00176903.2	Polymerase I and transcript release factor	PTRF	−3.8	3	21.5	1.7E−87	Involved in ribosomal RNA synthesis
IPI00909387.1	Growth hormone-inducible transmembrane protein	GHITM	−3.5	3	11.8	1.3E−09	Unknown function
IPI00219675.1	Ras-related C3 botulinum toxin substrate 1	RAC1	−3.4	8	23.7	2.4E−17	Small GTPase
IPI00016405.1	OCIA domain-containing protein 1	OCIAD1	−3.2	3	13.9	7.0E−05	Unknown function
IPI00018350.3	DNA replication licensing factor MCM5	MCM5	−3.0	6	3.4	3.4E−10	Involved in the initiation of DNA replication
IPI00141318.2	Cytoskeleton-associated protein 4	CKAP4	−3.0	4	25.9	2.9E−93	Type-II trans-membrane protein
IPI00328753.1	Kinectin	KTN1	−3.0	2	3.7	1.6E−13	Integral membrane protein
IPI00019385.3	Translocon-associated protein subunit δ	SSR4	−2.9	3	18.5	1.4E−15	Potential chaperone
IPI00300096.4	Ras-related protein Rab-35	RAB35	−2.7	43	32.3	3.9E−32	Involved in cytokinesis
IPI00639812.1	Microsomal glutathione *S*-transferase 3 variant	MGST3	−2.7	3	46.4	1.5E−88	Mediates inflammation
IPI00015077.1	Eukaryotic translation initiation factor 1	EIF1	−2.6	3	36.3	2.6E−23	Translation initiation
IPI00171573.2	Coiled-coil domain-containing protein 109A	CCDC109A	−2.6	2	9.1	8.3E−10	Membrane protein
IPI00797126.1	Putative uncharacterized protein NACA	NACA	−2.6	4	3.1	8.2E−09	Prevents inappropriate targeting of non-secretory polypeptides to the ER
IPI00215893.8	Heme oxygenase 1	HMOX1	−2.6	2	17.7	3.1E−13	Protects against oxidative stress. Promotes antiviral effect in HCV-infected cells [53]
IPI00796333.1	Fructose-bisphosphate aldolase A	ALDOA	−2.5	7	15.8	1.7E−63	Glycolytic enzyme
IPI00414676.6	Heat shock protein HSP 90-β	HSP90AB1	−2.5	4	13.7	4.7E−40	Involved in CpG-BODN-mediated anti-apoptotic response. May be present in HRSV particles [54]
IPI00016608.1	Transmembrane emp24 domain-containing protein 2	TMED2	−2.4	3	9	9.3E−06	Associated with budding of coated vesicles
IPI00216694.3	Plastin-3	PLS3	−2.4	2	4.4	0.01335	Actin binding protein
IPI00465290.3	DnaJ homolog subfamily C member 11	DNAJC11	−2.4	12	15.2	4.5E−48	Part of a large chaperone multi-protein complex
IPI00382843.1	Major prion protein	PRNP	−2.4	5	12.3	1.1E−05	Anchored at the cell membrane in rafts, potential role in oxidative burst compensation
IPI00140420.4	*Staphylococcal nuclease* domain-containing protein 1	SND1	−2.4	2	2.9	8.7E−05	Bridging factor between STAT6 and the basal transcription factor. Has roles in PIM1 regulation of MYB activity
IPI00011654.2	Tubulin β chain	TUBB	−2.4	11	41.2	3.2E−105	mRNA is upregulated at 4 and 24 h post-infection in RSV-infected cells [8]. Protein is increased 4.69-fold in RSV-infected cells [10]

Table 1. Continued

Protein IDs	Protein name	Gene name	RSV/Mock	Pep.	Seq. cov. (%)	PEP	Notes
IPI00028055.4	Transmembrane emp24 domain-containing protein 10	TMED10	−2.4	2	10.5	2.6E−12	Involved in endoplasmic reticulum stress response and potentially in the regulation of heat shock response and apoptosis
IPI00018146.1	14-3-3 protein theta	YWHAQ	−2.4	13	19.2	7.1E−22	Adapter protein
IPI00295992.4	ATPase family AAA domain-containing protein 3A	ATAD3A	−2.3	17	18.4	8.1E−21	Potentially involved in ATP binding
IPI00008524.1	Polyadenylate-binding protein 1	PABPC1	−2.3	16	19.3	1.8E−90	Binds to the poly(A) tail of mRNA, involved in translation initiation. PABP sequestered in the nucleus in Bunyamwera virus-infected cells [55]
IPI00887241.1	40S ribosomal protein S28	RPS28	−2.3	2	35.2	6.1E−09	Ribosomal protein
IPI00604590.3	Nucleoside diphosphate kinase	NME1-NME2	−2.2	12	32.9	1.3E−07	Involved in maintenance of concentrations of different nucleoside triphosphates
IPI00900293.1	Filamin B	FLNB	−2.2	10	43.9	0	Connects cells membrane constituents to the actin cytoskelton. Found in HRSV particles [54]
IPI00026111.3	Transmembrane and coiled-coil domain-containing protein 1	TMCO1	−2.2	2	12.2	1.2E−15	Unknown function
IPI00879004.1	DNA topoisomerase 2- α	TOP2A	−2.2	7	8.6	9.4E−44	Controls topological states of DNA
IPI00000874.1	Peroxiredoxin-1	PRDX1	−2.2	7	28.6	6.9E−15	Anti-oxidant
IPI00095891.2	Guanine nucleotide-binding protein G(s) subunit α isoforms Xlas	GNAS	−2.2	22	4.4	1.0E−13	Transducer in signalling systems
IPI00645446.1	cDNA FLJ59683, highly similar to Homo sapiens malignant T-cell amplified sequence 1 (MCTS1), mRNA	MCTS1	−2.1	4	15.9	1.8E−05	Potential RNA binding
IPI00374657.2	Putative uncharacterized protein VAPA	VAPA	−2.1	4	11.2	2.4E−07	Potential function in vesicle trafficking
IPI00219682.6	Erythrocyte band 7 integral membrane protein	STOM	−2.1	3	31.9	5.4E−114	Thought to regulate cation conductance
IPI00333215.1	Transcription elongation factor A protein 1	TCEA1	−2.0	6	7.3	1.8E−06	Necessary for RNA polymerase II transcription elongation
IPI00844388.1	Lymphoid-specific helicase	HELLS	−2.0	8	2.3	9.6E−05	Involved in cellular proliferation
IPI00218606.7	40S ribosomal protein S23	RPS23	−2.0	5	39.9	2.5E−10	Ribosomal protein
IPI00759776.1	ACTN1 protein	ACTN1	−2.0	6	49.5	0	F-actin cross-linking protein
IPI00396485.3	Elongation factor 1-α 1	EEF1A1	−2.0	2	31	2.1E−65	Elongation factor 2 (EEF2) decreased −4.37-fold in HRSV subgroup A infected cells [10]
IPI00409671.3	ATP-dependent RNA helicase DDX42	DDX42	−2.0	4	10.4	2.7E−28	RNA helicase
Cytoplasmic fraction – proteins that show increase abundance in RSV infected cells							
IPI00167949.6	Interferon-induced GTP-binding protein Mx1	MX1	+11	10	25.1	1.7E−241	MX2 mRNA is increased 1.4-fold at 24 h p.i. in HRSV subgroup A-infected cells [7]
IPI00018300.2	Interferon-induced protein with tetratricopeptide repeats 1	IFIT1	+8.9	2	20.7	1.8E−46	IFIT3 mRNA increased 2.8-fold at 24 h p.i. in HRSV subgroup A-infected cells [7]
IPI00030781.1	Signal transducer and activator of transcription 1-α/β	STAT1	+6.3	4	38.8	1.3E−155	mRNA is upregulated at 4 and 24 h p.i. in HRSV subgroup A-infected cells [8]
IPI00023673.1	Galectin-3-binding protein	LGALS3BP	+6.1	6	14.7	5.8E−44	May be involved in downregulation of IL-5

Table 1. Continued

Protein IDs	Protein name	Gene name	RSV/Mock	Pep.	Seq. cov. (%)	PEP	Notes
IPI00796379.2	β-2-microglobulin	B2M	+5.9	2	16.4	0.002381	Component of MHC class I
IPI00816252.1	Histone H2B type 2-E	HIST2H2BE	+4.4	17	20.6	3.6E−06	Core component of the nucleosome
IPI00744711.2	Polyribonucleotide nucleotidyltransferase 1, mitochondrial	PNPT1	+4.1	5	2.4	0.03691	Increased 10.85-fold in the total cell proteome of PIV-infected cells at 24 h p.i. [10]
IPI00642126.3	ALK lymphoma oligomerization partner on chromosome 17	KIAA1618	+3.6	5	3.7	1.4E−48	Unknown function
IPI00877174.1	cDNA FLJ78682, highly similar to Homo sapiens 2′-5′-oligoadenylate synthetase 3, 100 kDa (OAS3), mRNA; 2′-5′-oligoadenylate synthetase 3	OAS3	+3.5	2	3	0.00286	Also increased in the nuclear fraction. See above and it is also discussed in text
IPI00027252.6	Prohibitin-2	PHB2	+3.4	2	41.2	5.4E−127	Decreased in the mitochondrial proteins identified form the nuclear fraction. See above
IPI00017334.1	Prohibitin	PHB	+3.1	7	46.2	7.1E−64	Decreased in the nuclear fraction. See above
IPI00554788.5	Keratin, type I cytoskeletal 18	KRT18	+2.7	42	28.8	5.7E−272	Role in filament formation, associated with delivery of CFTR to the plasma membrane
IPI00295400.1	Tryptophanyl-tRNA synthetase, cytoplasmic	WARS	+2.6	3	10.8	2.6E−13	Involved in regulating ERK, Akt and eNOS pathways
IPI00856098.1	p180/ribosome receptor	RRBP1	+2.6	13	5.1	4.9E−11	Acts as a ribosome receptor and mediates the interaction between the ribosome and the ER
IPI00014898.3	Plectin-1	PLEC1	+2.5	10	0.7	0.000168	Links the cytoskeleton to the plasma membrane
IPI00748256.2	Putative uncharacterized protein PSME1	PSME1	+2.4	2	12.8	2.0E−05	Part of the proteasome
IPI00007188.5	ADP/ATP translocase 2	SLC25A5	+2.4	2	41.3	2.6E−46	Catalyzes the exchange of ADP and ATP across the inner mitochondrial membrane
IPI00291467.7	ADP/ATP translocase 3	SLC25A6	+2.4	5	47	2.4E−69	Catalyzes the exchange of ADP and ATP across the inner mitochondrial membrane
IPI00334190.4	Stomatin-like protein 2	STOML2	+2.4	2	8.7	0.06236	Involved in bridging polarized mitochondrial in the immunological synapse
IPI00006579.1	Cytochrome c oxidase subunit 4 isoform 1	COX4I1	+2.3	2	12.4	0.00668	Part of cytochrome c oxidase
IPI00022202.3	Phosphate carrier protein, mitochondrial	SLC25A3	+2.3	7	23.8	1.4E−22	Transport of phosphate groups from the cytosol to the mitochondrial matrix
IPI00216026.2	Voltage-dependent anion-selective channel protein 2	VDAC2	+2.2	8	7.1	1.5E−05	Forms a channel through the mitochondrial outer membrane and allows the diffusion of small hydrophilic molecules
IPI00871843.1	Protein-glutamine γ-glutamyltransferase 2	TGM2	+2.2	7	32.3	1.4E−113	Catalyzes the cross linking of proteins
IPI00007427.2	Anterior gradient protein 2 homolog	AGR2	+2.1	7	29.2	1.5E−15	Potential role in the secretion of mucus
IPI00216308.5	Voltage-dependent anion-selective channel protein 1	VDAC1	+2.1	4	16.6	2.1E−11	Forms a channel through the mitochondrial outer membrane and allows the diffusion of small hydrophilic molecules. Increased in abundance in *Scophthalmus maximus* Rhabdovirus-infected cells [56]

Table 1. Continued

Protein IDs	Protein name	Gene name	RSV/Mock	Pep.	Seq. cov. (%)	PEP	Notes
IPI00759776.1	ACTN1 protein	ACTN1	+2.1	3	20.8	1.1E−100	Decreased 2.65 and 2.85-fold in the total cell proteomes of hMPV and PIV infected cells, respectively, at 24 h p.i. [10]
IPI00847322.1	Superoxide dismutase	SOD2	+2.0	5	20.7	9.4E−06	Functions as an anti-oxidant. Potentially linked with ROS in HRSV subgroup A-infected cells [57]. mRNA increased in HRSV subgroup A-infected cells [36]. Protein induced in MV-infected cells [58]
IPI00337495.3	Procollagen-lysine, 2-oxoglutarate 5-dioxygenase 2	PLOD2	+2.0	2	4.4	5.2E−10	Involved in the stability of collagen cross-links
IPI00026154.3	Glucosidase 2 subunit β	PRKCSH	+2.0	3	9.7	2.4E−31	Regulatory subunit of glucosidase II
Nuclear fraction – mitochondrial proteins that show decreased abundance in RSV infected cells							
IPI00479905.5	NADH dehydrogenase [ubiquinone] 1 β subcomplex subunit 10	NDUFB10	−21.2	11	26.7	3.4E−11	Accessory subunit of the mitochondrial membrane respiratory chain NADH dehydrogenase (Complex I)
IPI00797738.1	Cytochrome c oxidase subunit 6B1	COX6B1	−18.2	3	27.2	3.4E−07	Component of the ubiquinol-cytochrome c reductase complex
IPI00790644.1	Cytochrome b-c1 complex subunit 7	UQCRB	−18.0	4	25	2.6E−24	Component of the ubiquinol-cytochrome c reductase complex
IPI00216026.2	Voltage-dependent anion-selective channel protein 2	VDAC2	−18.0	9	60.2	5.2E−136	Forms a channel through the mitochondrial outer membrane and allows the diffusion of small hydrophilic molecules
IPI00554701.2	Cytochrome b-c1 complex subunit 9	UQCR10	−16.5	6	50.8	2.2E−33	Component of the ubiquinol-cytochrome c reductase complex
IPI00296022.1	Cytochrome b-c1 complex subunit 6, mitochondrial	UQCRH	−15.7	2	29.7	1.6E−19	Component of the ubiquinol-cytochrome c reductase complex
IPI00216308.5	Voltage-dependent anion-selective channel protein 1	VDAC1	−15.6	4	80.6	0	Forms a channel through the mitochondrial outer membrane and allows the diffusion of small hydrophilic molecules
IPI00031804.1	Voltage-dependent anion-selective channel protein 3	VDAC3	−15.4	2	50.2	5.2E−109	Forms a channel through the mitochondrial outer membrane and allows the diffusion of small hydrophilic molecules
IPI00219729.3	Mitochondrial 2-oxoglutarate/malate carrier protein	SLC25A11	−15.4	3	11.5	2.3E−32	Catalyzes the transport of 2-oxoglutarate across the inner mitochondrial membrane
IPI00014053.3	Mitochondrial import receptor subunit TOM40 homolog	TOMM40	−14.1	3	54	3.3E−163	Channel-forming protein essential of import of protein precursors into mitochondria. Potential anti-viral effect in African swine fever virus infected cells [59]
IPI00646556.1	NADH dehydrogenase [ubiquinone] flavoprotein 2, mitochondrial	NDUFV2	−12.7	3	22.2	4.2E−15	Part of Complex I
IPI00027252.6	Prohibitin-2	PHB2	−12.6	2	42.5	9.8E−101	Mediates transcriptional repression.
IPI00219685.5	NADH dehydrogenase [ubiquinone] 1 α subcomplex subunit 13	YJEFN3	−12.4	3	19.8	1.9E−07	Accessory subunit of Complex I
IPI00010845.3	NADH dehydrogenase [ubiquinone] iron-sulfur protein 8, mitochondrial	NDUFS8	−12.3	2	14.3	1.3E−09	Core subunit of Complex I
IPI00291467.7	ADP/ATP translocase 3	SLC25A6	−11.1	2	37.9	4.2E−86	Catalyzes the exchange of ADP and ATP across the inner mitochondrial membrane. Increased in the cytoplasmic fraction
IPI00883602.1	Cytochrome b-c1 complex subunit Rieske, mitochondrial	UQCRFS1	−10.1	4	21.5	4.5E−39	Component of the ubiquinol-cytochrome c reductase complex

Table 1. Continued

Protein IDs	Protein name	Gene name	RSV/Mock	Pep.	Seq. cov. (%)	PEP	Notes
IPI00006579.1	Cytochrome c oxidase subunit 4 isoform 1, mitochondrial	COX4I1	−9.6	2	46.2	7.9E−48	Component of cytochrome c oxidase
IPI00220059.5	NADH dehydrogenase [ubiquinone] 1 β subcomplex subunit 4	NDUFB4	−8.8	3	31.8	4.8E−50	Accessory subunit of Complex I
IPI00007188.5	ADP/ATP translocase 2	SLC25A5	−8.5	4	44.6	4.8E−97	Catalyzes the exchange of ADP and ATP across the inner mitochondrial membrane. Increased in the cytoplasmic fraction
IPI00103509.4	NADH dehydrogenase ubiquinone 1 α subcomplex	NDUFA10 (includes EG:4705)	−8.4	10	7.2	3.4E−07	Non-catalytic component of Complex I
IPI00025796.3	NADH dehydrogenase [ubiquinone] iron-sulfur protein 3, mitochondrial	NDUFS3	−8.1	2	28.8	4.6E−47	Core subunit of Complex I
IPI00334190.4	Stomatin-like protein 2	STOML2	−8.0	5	30.3	1.6E−168	Involved in bridging polarized mitochondrial in the immunological synapse
IPI00554681.2	NADH dehydrogenase [ubiquinone] 1 α subcomplex subunit 5	NDUFA5	−7.8	7	44	8.9E−96	Accessory subunit of Complex I
IPI00013847.4	Cytochrome b-c1 complex subunit 1, mitochondrial	UQCRC1	−7.6	3	33.8	2.3E−205	Component of the ubiquinol-cytochrome c reductase complex
IPI00028520.2	NADH dehydrogenase [ubiquinone] flavoprotein 1, mitochondrial	NDUFV1	−7.4	3	19.8	3.6E−15	Core subunit of Complex I
IPI00007084.2	Calcium-binding mitochondrial carrier protein Aralar2	SLC25A13	−7.2	3	10.2	1.3E−12	Calcium-dependent mitochondrial aspartate and glutamate carrier
IPI00016676.1	Mitochondrial import receptor subunit TOM20 homolog	TOMM20	−6.4	2	13.1	6.5E−06	Together with TOM22 functions as the transit peptide receptor at the surface of the mitochondrial outer membrane
IPI00028883.1	NADH dehydrogenase [ubiquinone] 1 β subcomplex subunit 8, mitochondrial	NDUFB8	−6.4	3	25.3	5.3E−24	Accessory subunit of Complex I
IPI00219385.3	NADH dehydrogenase [ubiquinone] 1 β subcomplex subunit 6	NDUFB6	−5.9	2	32	1.3E−13	Accessory subunit of Complex I
IPI00294159.3	Tricarboxylate transport protein, mitochondrial	SLC25A1	−5.6	2	12.5	9.4E−10	Involved in citrate-H(+)/ malate exchange
IPI00013195.1	39S ribosomal protein L49, mitochondrial	MRPL49	−5.6	2	23.5	2.0E−11	Component of the mitochondrial ribosome
IPI00003968.1	NADH dehydrogenase [ubiquinone] 1 α subcomplex subunit 9, mitochondrial	DUFA9 (includes EG:4704)	−5.4	3	11.9	5.1E−21	Accessory subunit of complex I
IPI00012855.1	Transmembrane protein 11	TMEM11	−5.0	2	12.5	1.6E−05	Putative receptor protein
IPI00386258.1	Mitochondrial carrier homolog 1	MTCH1	−4.9	5	8	1.7E−15	Potential mitochondrial transporter

Table 1. Continued

Protein IDs	Protein name	Gene name	RSV/Mock	Pep.	Seq. cov. (%)	PEP	Notes
IPI00021805.1	Microsomal glutathione *S*-transferase 1	MGST1	−4.6	3	27.1	1.1E−57	Conjugation of reduced glutathione to exogenous and endogenous hydrophobic electrophiles. Glutathione *S*-transferase 1 mRNA decreased in HRSV subgroup A-infected cells [36]
IPI00215777.1	Phosphate carrier protein, mitochondrial	SLC25A3	−4.2	7	26	6.9E−21	Transport of phosphate groups from the cytosol to the mitochondrial matrix
IPI00015602.1	Mitochondrial import receptor subunit TOM70	TOMM70A	−3.9	3	8.6	5.8E−06	Accelerates import of mitochondrial precursor proteins
IPI00472939.2	Signal peptidase complex subunit 2	SPCS2	−3.9	6	12.8	1.1E−11	Component of the microsomal signal peptidase complex
IPI00788907.2	Phosphoglycerate mutase family member 5	PGAM5	−3.8	3	13.8	6.2E−06	Involved in glycolysis
IPI00440493.2	ATP synthase subunit α, mitochondrial	ATP5A1	−3.4	6	7.1	3.8E−05	Mitochondrial protein producing ATP from ADP
IPI00307749.2	NADH dehydrogenase [ubiquinone] iron-sulfur protein 7, mitochondrial	NDUFS7	−3.2	4	6.4	2.5E−08	Core subunit of Complex I
IPI00337494.7	Calcium-binding mitochondrial carrier protein SCaMC-1	SLC25A24	−3	15	4.6	2.0E−05	Calcium-dependent mitochondrial solute carrier
IPI00009960.6	Mitochondrial inner membrane protein	IMMT	−2.7	6	21.1	2.2E−79	Cell proliferation
IPI00007611.1	ATP synthase subunit O, mitochondrial	ATP5O	−2.6	3	13.1	2.3E−18	Produces ATP from ADP
IPI00640747.3	Putative mitochondrial import inner membrane translocase subunit Tim23B	TIMM23B	−2.0	9	22.6	6.9E−45	Potential role of translocation of transit containing proteins across the mitochondrial inner membrane

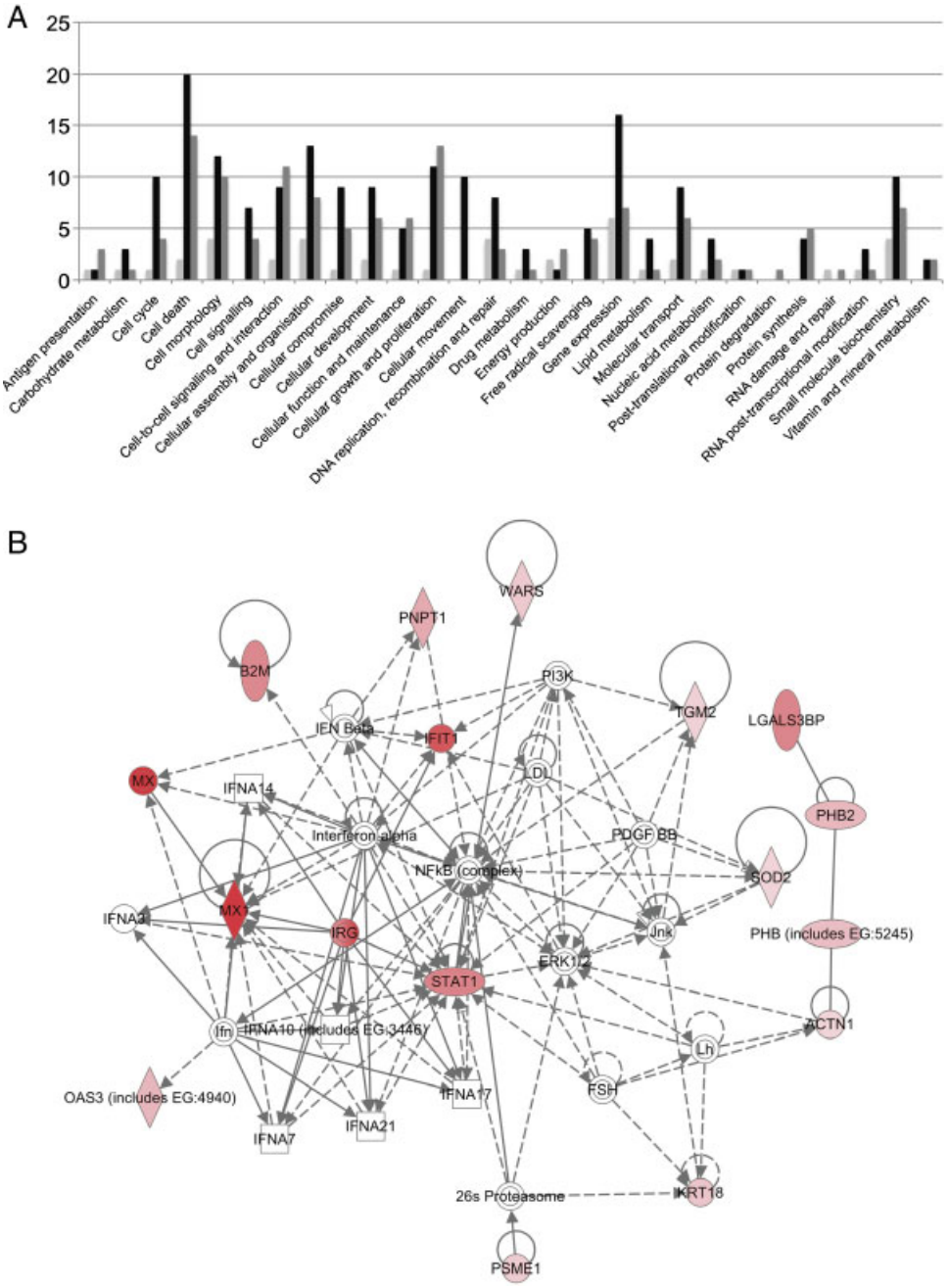

Figure 1. (A) Ingenuity Pathway Analysis of two or more fold differentially expressed proteins in HRSV subgroup B-infected A549 cells. Proteins are grouped into different functional categories (*x*-axis) with the *y*-axis showing numbers of proteins in each group. These represent differentially expressed proteins from the nuclear fraction (twofold or less in light gray shading, twofold or more in black) and the cytoplasic fraction (twofold or more in heavy gray shading). The definitions of each functional class are described in Supporting Information Table 3. (B) Network pathway analysis. Proteins shaded in red indicate a twofold or more increase in abundance in the cytoplasmic fraction of RSV-infected cells compared with mock-infected cells and the color intensity corresponds to the degree of abundance. Proteins in white are those identified through the Ingenuity Knowledge Base. The shapes denote the molecular class of the protein. A solid line indicates a direct molecular interaction and a dashed line indicates an indirect molecular interaction. A full explanation of lines and relationships is provided in Supporting Information Fig. 4.

reflected the quantitative proteomic data analysis (Fig. 2). Notably, in the immunofluorescence analysis of mock-infected cells, VDAC1 is present in the nucleus and cytoplasm but in HRSV-infected cells VDAC1 appeared to be absent from nuclear compartment by 24 h (Fig. 2). This reflects the quantitative proteomic analysis, which measured an approximately 16-fold decrease of VDAC1 in the nuclear fraction and approximately twofold increase in VDAC1 in the cytoplasmic fraction prepared from HRSV-infected cells compared with mock-infected cells. Curiously, as discussed, many of the mitochondrial proteins were identified in the nuclear fraction. Independent reports of nuclear fractions obtained from A549 cells (prepared by a different method) also contained mitochondrial proteins, which were suggested to be a potential contaminant [22], and has also been documented in the purification of nucleoli from the nucleus [45]. However, tubular structures that contain mitochondria can be found projecting into the nucleus [46] and may thus explain the presence of (some) mitochondrial proteins in nuclear factions.

Several other proteins of interest were used to validate the data set and may also indicate that cut-off values lower

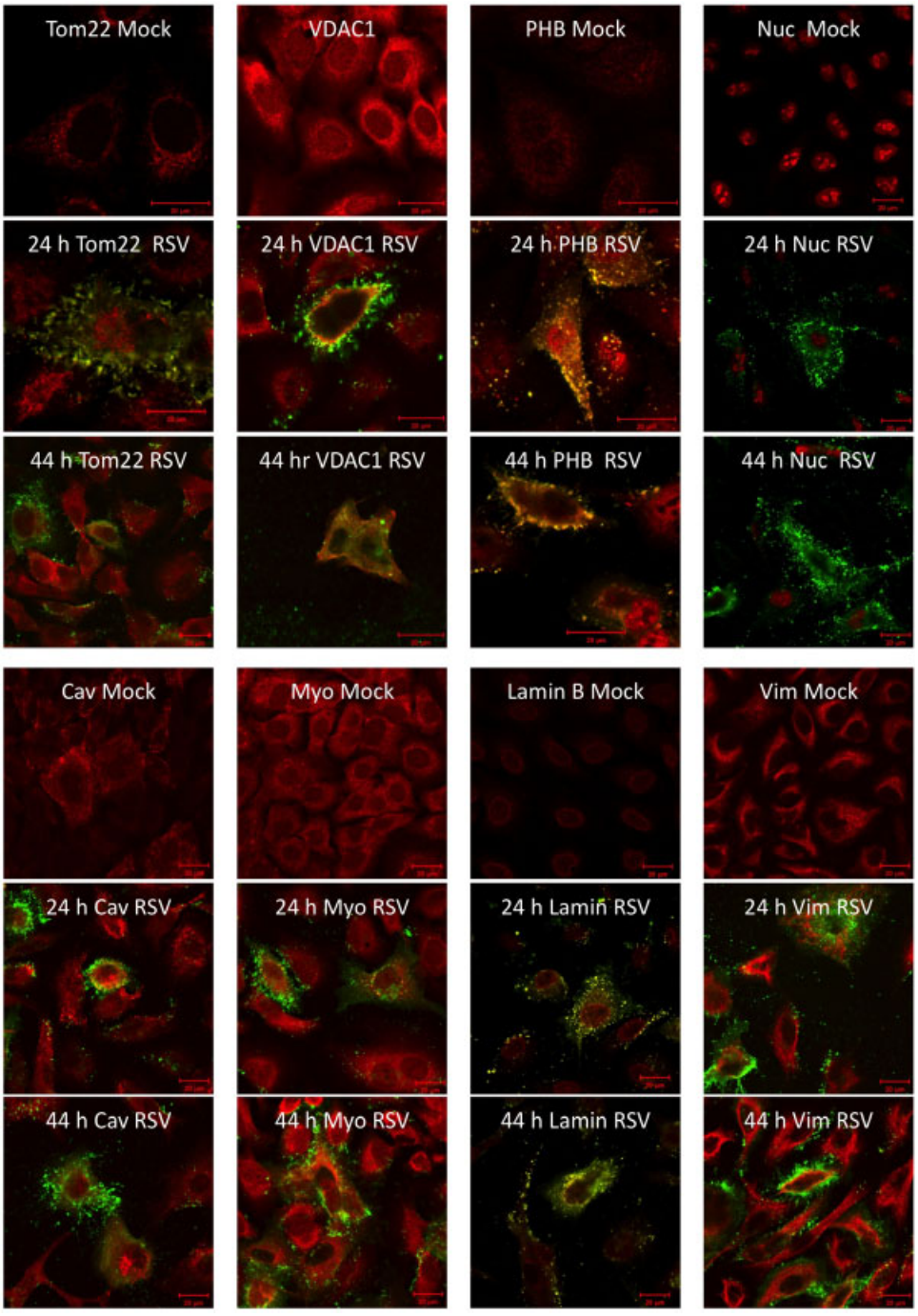

Figure 2. Indirect immunofluorescence confocal microscopy analysis of cellular protein localization, in mock-infected and HRSV-infected A549 cells 24 and 44 h post-infection. Tom22, VDAC1, PHB, nucleolin (Nuc), lamin, vimentin (Vim), myosin6 (Myo) and caveolin (Cav) are stained red; HRSV proteins are shown in green. Merged images are presented. The scale bar is 20 μm.

than 2.0-fold could be considered. For example, in the quantitative proteomic analysis, nucleolin was shown to decrease 1.6-fold in the nuclear fraction prepared from HRSV-infected cells, compared with mock-infected cells, a result validated using immunoblot analysis (Supporting Information Fig. 1). Indirect immunofluorescence confocal microscopy revealed that nucleolin was absent from the nucleus/nucleolus of some infected cells at 24 h post-infection and from all infected cells at 44 h post-infection (example images are shown in Fig. 2). Nucleolin was also reported to be decreased at 24 h post-infection in A549 cells infected with human metapneumovirus [10].

In the quantitative proteomic analysis, caveolin was increased 1.7-fold in the cytoplasmic fraction prepared from HRSV-infected cells, compared with mock-infected cells. Again, examples could be found using indirect immunofluorescence confocal microscopy where the relative fluorescence of caveolin was greater in HRSV-infected cells

compared with mock-infected cells (Fig. 2). No significant change in the abundance of myosin 6 or lamin B was identified by either the quantitative proteomic analysis or by indirect immunofluorescence confocal microscopy (Fig. 2).

The quantitative proteomic analysis indicated that proteome changes in response to infection were not global, but confined to specific proteins or protein classes. This is similar to a recent temporal 2-DE comparison of the interaction of HRSV subgroup A and other respiratory viruses belonging to the *Paramyxoviridae* with A549 cells [10]. Here, based on this analysis, van Diepen *et al.* [10] proposed four processes in virus-induced apoptosis: virus uptake and infection, stress response, disruption of cellular structures and cell death by apoptosis. The quantitative proteomic analysis conducted here would support this hypothesis, particularly with regard to disruption of mitochondria and nucleoli, the latter of which has been observed in proteomic analysis of other virus-infected cells [18, 19, 27]. Such changes may have functional consequences for host-cell biology. For example, nucleolin is a major constituent of the nucleolus and functions as a possible hub protein [47]. Therefore, changes to the abundance of this protein may have consequences for nucleolar function [48, 49].

Overall, the analysis demonstrates how the application of SILAC coupled to LC-MS/MS for identification and quantification, and bioinformatic analysis can be readily used to study the interaction of viruses with the cellular proteome. In this case, the relatively unstudied HRSV subgroup B virus has been shown to alter the abundance of proteins involved in the regulation of specific host-cell pathways.

Cellular and viral proteins were identified and quantified in the nuclear and cytoplasmic fractions and raw data sets were deposited in the Proteomics Identifications Database (PRIDE) using the PRIDE convertor tool. (Accession nos. 13270 for the cytoplasm and 13269 for the nucleus).

This research was supported by an MRC studentship awarded to D.C.M. J.A.H. is a Leverhulme Trust Research Fellow and J.N.B. is a Research Council UK Fellow. Dr. Patricia Cane (Health Protection Agency) is thanked for the provistion of the HRSV subgroup B strain used in this study. Edward Emmott and Weining Wu are thanked for their help with various aspects of the study. Dr. Paul Ajuh at Dundee Cell Products is thanked for help with interpretation of the quantitative proteomic analysis.

The authors have declared no conflict of interest.

References

[1] Hall, C. B., Weinberg, G. A., Iwane, M. K., Blumkin, A. K. *et al.*, The burden of respiratory syncytial virus infection in young children. *N. Engl. J. Med.* 2009, *360*, 588–598.

[2] Bermingham, A., Collins, P. L., The M2-2 protein of human respiratory syncytial virus is a regulatory factor involved in the balance between RNA replication and transcription. *Proc. Natl. Acad. Sci. USA* 1999, *96*, 11259–11264.

[3] Carter, S. D., Dent, K. C., Atkins, E., Foster, T. L. *et al.*, Direct visualization of the small hydrophobic protein of human respiratory syncytial virus reveals the structural basis for membrane permeability. *FEBS Lett.* 2010, *584*, 2786–2790.

[4] Whitehead, S. S., Hill, M. G., Firestone, C. Y., St Claire, M. *et al.*, Replacement of the F and G proteins of respiratory syncytial virus (RSV) subgroup A with those of subgroup B generates chimeric live attenuated RSV subgroup B vaccine candidates. *J. Virol.* 1999, *73*, 9773–9780.

[5] Nokes, J. D., Cane, P. A., New strategies for control of respiratory syncytial virus infection. *Curr. Opin. Infect. Dis.* 2008, *21*, 639–643.

[6] Collins, P. L., Graham, B. S., Viral and host factors in human respiratory syncytial virus pathogenesis. *J. Virol.* 2008, *82*, 2040–2055.

[7] Martinez, I., Lombardia, L., Garcia-Barreno, B., Dominguez, O., Melero, J. A., Distinct gene subsets are induced at different time points after human respiratory syncytial virus infection of A549 cells. *J. Gen. Virol.* 2007, *88*, 570–581.

[8] Huang, Y. C., Li, Z., Hyseni, X., Schmitt, M. *et al.*, Identification of gene biomarkers for respiratory syncytial virus infection in a bronchial epithelial cell line. *Genomic Med.* 2008, *2*, 113–125.

[9] Brasier, A. R., Spratt, H., Wu, Z., Boldogh, I. *et al.*, Nuclear heat shock response and novel nuclear domain 10 reorganization in respiratory syncytial virus-infected a549 cells identified by high-resolution two-dimensional gel electrophoresis. *J. Virol.* 2004, *78*, 11461–11476.

[10] van Diepen, A., Brand, H. K., Sama, I., Lambooy, L. H. *et al.*, Quantitative proteome profiling of respiratory virus-infected lung epithelial cells. *J. Proteomics* 2010, *73*, 1680–1693.

[11] Gibbs, J. D., Ornoff, D. M., Igo, H. A., Zeng, J. Y., Imani, F., Cell cycle arrest by transforming growth factor beta1 enhances replication of respiratory syncytial virus in lung epithelial cells. *J. Virol.* 2009, *83*, 12424–12431.

[12] Yeo, D. S., Chan, R., Brown, G., Ying, L. *et al.*, Evidence that selective changes in the lipid composition of raft-membranes occur during respiratory syncytial virus infection. *Virology* 2009, *386*, 168–182.

[13] Swedan, S., Musiyenko, A., Barik, S., Respiratory syncytial virus nonstructural proteins decrease levels of multiple members of the cellular interferon pathways. *J. Virol.* 2009, *83*, 9682–9693.

[14] Choudhary, S., Boldogh, S., Garofalo, R., Jamaluddin, M., Brasier, A. R., Respiratory syncytial virus influences NF-kappaB-dependent gene expression through a novel pathway involving MAP3K14/NIK expression and nuclear complex formation with NF-kappaB2. *J. Virol.* 2005, *79*, 8948–8959.

[15] Thomas, K. W., Monick, M. M., Staber, J. M., Yarovinsky, T. *et al.*, Respiratory syncytial virus inhibits apoptosis and induces NF-kappa B activity through a phosphatidylinositol 3-kinase-dependent pathway. *J. Biol. Chem.* 2002, *277*, 492–501.

[16] Murawski, M. R., Bowen, G. N., Cerny, A. M., Anderson, L. J. *et al.*, Respiratory syncytial virus activates innate immunity through Toll-like receptor 2. *J. Virol.* 2009, *83*, 1492–1500.

[17] Martinez, I., Lombardia, L., Garcia-Barreno, B., Dominguez, O., Melero, J. A., Distinct gene subsets are induced at different time points after human respiratory syncytial virus infection of A549 cells. *J. Gen. Virol.* 2007, *88*, 570–581.

[18] Emmott, E., Rodgers, M., Macdonald, M., McCrory, S. *et al.*, Quantitative proteomics using stable isotope labeling with amino acids in cell culture (SILAC) reveals changes in the cytoplasmic, nuclear and nucleolar proteomes in Vero cells infected with the coronavirus infectious bronchitis virus. *Mol. Cell. Proteomics* 2010, *9*, 1920–1936.

[19] Emmott, E., Smith, C., Emmett, S. R., Dove, B. K., Hiscox, J. A., Elucidation of the avian nucleolar proteome by quantitative proteomics using stable isotope labeling with amino acids in cell culture (SILAC) and alteration in the coronavirus infectious bronchitis virus infected cells. *Proteomics* 2010, *10*, 3558–3562.

[20] Vester, D., Rapp, E., Gade, D., Genzel, Y., Reichl, U., Quantitative analysis of cellular proteome alterations in human influenza A virus-infected mammalian cell lines. *Proteomics* 2009, *9*, 3316–3327.

[21] Ciotti, M., Marzano, V., Giuliani, L., Nuccetelli, M. *et al.*, Proteomic investigation in A549 lung cell line stably infected by HPV16E6/E7 oncogenes. *Respiration* 2009, *77*, 427–439.

[22] Forbus, J., Spratt, H., Wiktorowicz, J., Wu, Z. *et al.*, Functional analysis of the nuclear proteome of human A549 alveolar epithelial cells by HPLC-high resolution 2-D gel electrophoresis. *Proteomics* 2006, *6*, 2656–2672.

[23] Kotelkin, A., Prikhod'ko, E. A., Cohen, J. I., Collins, P. L., Bukreyev, A., Respiratory syncytial virus infection sensitizes cells to apoptosis mediated by tumor necrosis factor-related apoptosis-inducing ligand. *J. Virol.* 2003, *77*, 9156–9172.

[24] Lindemans, C. A., Coffer, P. J., Schellens, I. M., de Graaff, P. M. *et al.*, Respiratory syncytial virus inhibits granulocyte apoptosis through a phosphatidylinositol 3-kinase and NF-kappaB-dependent mechanism. *J. Immunol.* 2006, *176*, 5529–5537.

[25] Cox, J., Mann, M., MaxQuant enables high peptide identification rates, individualized p.p.b.-range mass accuracies and proteome-wide protein quantification. *Nat. Biotechnol.* 2008, *26*, 1367–1372.

[26] Mann, M., Functional and quantitative proteomics using SILAC. *Nat. Rev. Mol. Cell. Biol.* 2006, *7*, 952–958.

[27] Lam, Y. W., Evans, V. C., Heesom, K. J., Lamond, A. I., Matthews, D. A., Proteomics analysis of the nucleolus in adenovirus-infected cells. *Mol. Cell. Proteomics* 2009, *9*, 117–130.

[28] Vizcaino, J. A., Cote, R., Reisinger, F., Foster, J. M. *et al.*, A guide to the Proteomics Identifications Database proteomics data repository. *Proteomics* 2009, *9*, 4276–4283.

[29] Barsnes, H., Vizcaino, J. A., Eidhammer, I., Martens, L., PRIDE converter: making proteomics data-sharing easy. *Nat. Biotechnol.* 2009, *27*, 598–599.

[30] Liu, N., Song, W., Wang, P., Lee, K. *et al.*, Proteomics analysis of differential expression of cellular proteins in response to avian H9N2 virus infection in human cells. *Proteomics* 2008, *8*, 1851–1858.

[31] Chan, E. Y., Qian, W. J., Diamond, D. L., Liu, T. *et al.*, Quantitative analysis of human immunodeficiency virus type 1-infected CD4+ cell proteome: dysregulated cell cycle progression and nuclear transport coincide with robust virus production. *J. Virol.* 2007, *81*, 7571–7583.

[32] Young, D. F., Didcock, L., Goodbourn, S., Randall, R. E., Paramyxoviridae use distinct virus-specific mechanisms to circumvent the interferon response. *Virology* 2000, *269*, 383–390.

[33] Pletneva, L. M., Haller, O., Porter, D. D., Prince, G. A., Blanco, J. C., Induction of type I interferons and interferon-inducible Mx genes during respiratory syncytial virus infection and reinfection in cotton rats. *J. Gen. Virol.* 2008, *89*, 261–270.

[34] Johnson, T. R., Mertz, S. E., Gitiban, N., Hammond, S. *et al.*, Role for innate IFNs in determining respiratory syncytial virus immunopathology. *J. Immunol.* 2005, *174*, 7234–7241.

[35] Jamaluddin, M., Tian, B., Boldogh, I., Garofalo, R. P., Brasier, A. R., Respiratory syncytial virus infection induces a reactive oxygen species-MSK1-phospho-Ser-276 RelA pathway required for cytokine expression. *J. Virol.* 2009, *83*, 10605–10615.

[36] Hosakote, Y. M., Liu, T., Castro, S. M., Garofalo, R. P., Casola, A., Respiratory syncytial virus induces oxidative stress by modulating antioxidant enzymes. *Am. J. Respir. Cell. Mol. Biol.* 2009, *41*, 348–357.

[37] Desterro, J. M., Keegan, L. P., Lafarga, M., Berciano, M. T. *et al.*, Dynamic association of RNA-editing enzymes with the nucleolus. *J. Cell. Sci.* 2003, *116*, 1805–1818.

[38] Tenoever, B. R., Ng, S. L., Chua, M. A., McWhirter, S. M. *et al.*, Multiple functions of the IKK-related kinase IKKepsilon in interferon-mediated antiviral immunity. *Science* 2007, *315*, 1274–1278.

[39] Ngamurulert, S., Limjindaporn, T., Auewaraku, P., Identification of cellular partners of Influenza A virus (H5N1) nonstructural protein NS1 by yeast two-hybrid system. *Acta Virol.* 2009, *53*, 153–159.

[40] Toth, A. M., Li, Z., Cattaneo, R., Samuel, C. E., RNA-specific adenosine deaminase ADAR1 suppresses measles virus-induced apoptosis and activation of protein kinase PKR. *J. Biol. Chem.* 2009, *284*, 29350–29356.

[41] Nie, Y., Hammond, G. L., Yang, J. H., Double-stranded RNA deaminase ADAR1 increases host susceptibility to virus infection. *J. Virol.* 2007, *81*, 917–923.

[42] Mashimo, T., Simon-Chazottes, D., Guenet, J. L., Innate resistance to flavivirus infections and the functions of 2′-5′

oligoadenylate synthetases. *Curr. Top. Microbiol. Immunol.* 2008, *321*, 85–100.

[43] Kajaste-Rudnitski, A., Mashimo, T., Frenkiel, M. P., Guenet, J. L. *et al.*, The 2′,5′-oligoadenylate synthetase 1b is a potent inhibitor of West Nile virus replication inside infected cells. *J. Biol. Chem.* 2006, *281*, 4624–4637.

[44] Behera, A. K., Kumar, M., Lockey, R. F., Mohapatra, S. S., 2′-5′ Oligoadenylate synthetase plays a critical role in interferon-gamma inhibition of respiratory syncytial virus infection of human epithelial cells. *J. Biol. Chem.* 2002, *277*, 25601–25608.

[45] Ahmad, Y., Boisvert, F. M., Gregor, P., Cobley, A., Lamond, A. I., NOPdb: Nucleolar Proteome Database—2008 update. *Nucleic Acids Res.* 2009, *37*, D181–184.

[46] Lui, P. P., Chan, F. L., Suen, Y. K., Kwok, T. T., Kong, S. K., The nucleus of HeLa cells contains tubular structures for Ca2+ signaling with the involvement of mitochondria. *Biochem. Biophys. Res. Commun.* 2003, *308*, 826–833.

[47] Emmott, E., Hiscox, J. A., Nucleolar targetting: the hub of the matter. *EMBO Rep.* 2009, *10*, 231–238.

[48] Hiscox, J. A., RNA viruses: hijacking the dynamic nucleolus. *Nat. Rev. Microbiol.* 2007, *5*, 119–127.

[49] Hiscox, J. A., Whitehouse, A., Matthews, D. A., Nucleolar proteomics and viral infection. *Proteomics* 2010, *10*, doi: 10.1002/pmic.201000251.

[50] Janssen, R., Pennings, J., Hodemaekers, H., Buisman, A. *et al.*, Host transcription profiles upon primary respiratory syncytial virus infection. *J. Virol.* 2007, *81*, 5958–5967.

[51] Stefanovic, S., Windsor, M., Nagata, K. I., Inagaki, M., Wileman, T., Vimentin rearrangement during African swine fever virus infection involves retrograde transport along microtubules and phosphorylation of vimentin by calcium calmodulin kinase II. *J. Virol.* 2005, *79*, 11766–11775.

[52] Bao, X., Sinha, M., Liu, T., Hong, C. *et al.*, Identification of human metapneumovirus-induced gene networks in airway epithelial cells by microarray analysis. *Virology* 2008, *374*, 114–127.

[53] Lehmann, E., El-Tantawy, W. H., Ocker, M., Bartenschlager, R. *et al.*, The heme oxygenase 1 product biliverdin interferes with hepatitis C virus replication by increasing antiviral interferon response. *Hepatology* 2010, *51*, 398–404.

[54] Radhakrishnan, A., Yeo, D., Brown, G., Myaing, M. Z. *et al.*, Protein analysis of purified respiratory syncytial virus particles reveals an important role for heat shock protein 90 in virus particle assembly. *Mol. Cell. Proteomics* 2010, *9*, 1829–1848

[55] Blakqori, G., van Knippenberg, I., Elliott, R. M., Bunyamwera orthobunyavirus S-segment untranslated regions mediate poly(A) tail-independent translation. *J. Virol.* 2009, *83*, 3637–3646.

[56] Lu, A. J., Dong, C. W., Du, C. S., Zhang, Q. Y., Characterization and expression analysis of Paralichthys olivaceus voltage-dependent anion channel (VDAC) gene in response to virus infection. *Fish Shellfish Immunol.* 2007, *23*, 601–613.

[57] Liu, T., Castro, S., Brasier,A. R., Jamaluddin, M. *et al.*, Reactive oxygen species mediate virus-induced STAT activation: role of tyrosine phosphatases. *J. Biol. Chem.* 2004, *279*, 2461–2469.

[58] Wang, M., Howell, J. M., Libbey, J. E., Tainer, J. A., Fujinami, R. S., Manganese superoxide dismutase induction during measles virus infection. *J. Med. Virol.* 2003, *70*, 470–474.

[59] Chang, A. C., Zsak, L., Feng, Y., Mosseri, R. *et al.*, Phenotype-based identification of host genes required for replication of African swine fever virus. *J. Virol.* 2006, *80*, 8705–8717.

